Chemically Recyclable Linear and Branched Polyethylenes Synthesized from Stoichiometrically Self-balanced Telechelic Polyethylenes

Yoon-Jung Jang, Sam Nguyen, and Marc A. Hillmyer*

Department of Chemistry, University of Minnesota, Minneapolis, MN 55455, USA

*Corresponding author (e-mail: hillmyer@umn.edu)

Abstract

High-density polyethylene (HDPE) is a widely used commercial plastic due to its excellent mechanical properties, chemical resistance, and water vapor barrier properties. However, less than 10% of HDPE is mechanically recycled, and chemical recycling of HDPE is challenging due to inherent strength of the carbon-carbon backbone bonds. Here, we report chemically recyclable linear and branched HDPE with sparce backbone ester groups synthesized from transesterification of telechelic polyethylene macromonomers. Stoichiometrically self-balanced telechelic polyethylenes underwent transesterification polymerization to produce the PE-ester samples with high number average molar masses up to 111 kg/mol. Moreover, transesterification polymerization of the telechelic polyethylenes and the multifunctional diethyl 5-(hydroxymethyl)isophthalate generated branched PE-esters. Thermal and mechanical properties of the PE-esters were comparable to commercial HDPE and tunable through control of the ester content in the backbone. In addition, branched PE-esters showed higher levels of melt-strain hardening compared to linear versions. The PE-ester was depolymerized into telechelic macromonomers through straightforward methanolysis and the resulting macromonomers could be effectively repolymerized to generate high molar mass recycled PE-ester samples. This is a new and promising method for synthesizing and recycling high-molar-mass linear and branched PE-esters, which are competitive with HDPE and have easily tailorable properties.

Introduction

Polyolefins are widely used for automotive parts, furniture, packaging materials, and myriad of other applications.[1–3] Nearly 180 million metric tons of polyolefins were produced in 2018;[4–7] 47 million metric tons of which was high-density polyethylene (HDPE). Chemical resistance, ease of processability, high toughness, and low water vapor permeability are all

attractive attributes of HDPE that drive broad implementation.[8] While hydrophobicity, crystallinity, and high bond strength of the carbon-carbon bond in HDPE contribute to its attractive material properties, these features largely prevent degradation in the environment.[9] Less than 10% of HDPE was recycled in 2018, and most HDPE was incinerated or sent to landfills at the end of use.[6,10,11]

The design of polymeric materials with enhanced degradability or chemical recyclability while maintaining attractive properties is of contemporary interest.[12–35] Chemical structures of such polymers mimic polyethylene with cleavable chemical bonds in the backbone, such as ester groups.[14–16,18,22,24–34] For example, in a pioneering study, Häußler *et al*. prepared polyethylene-like materials with 16 or 18 CH_2 groups between ester bonds.[18] The polymers were prepared through step-growth polycondensation of diesters and diols with long-chain alkyl moieties (Scheme 1A). Mechanical properties of the materials were competitive to commercial HDPE, and they were depolymerized back into monomers in methanol. However, their melting temperature was 99 °C, which is significantly lower than that of HDPE (132 °C) and could compromise use in some applications.

Scheme 1. Approaches to Synthesize Chemically Recyclable Polyethylenes

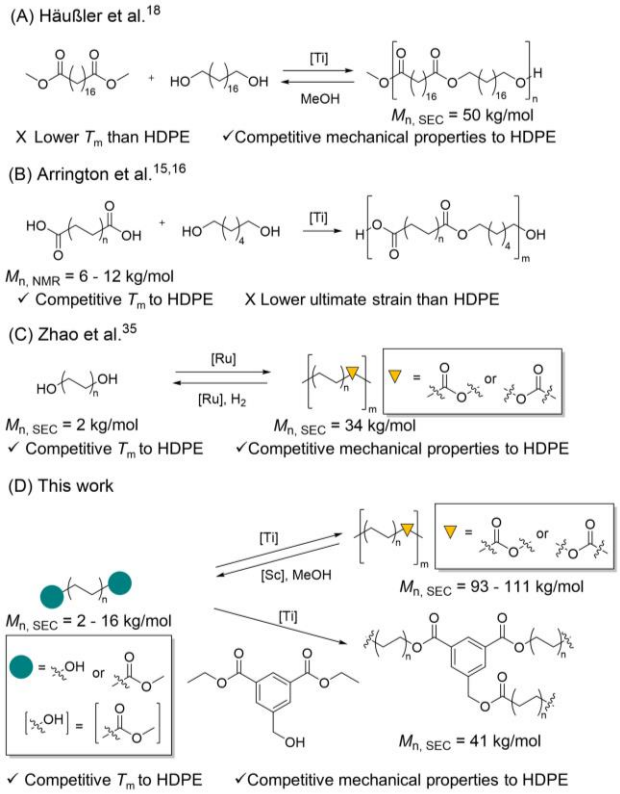

Longer spacing between ester linkages can lead to comparable thermal and mechanical properties of such chemically recyclable polymers to HDPE. These materials can be prepared through step-growth polymerization of telechelic macromonomers. Recently, Kocen *et al*. demonstrated the synthesis of chemically recyclable ester-linked polypropylene from isotactic polypropylene with unsaturated alkene groups in the main chain.[14] The polymer exhibited competitive mechanical properties to linear low density polyethylene. Arrington *et al*. reported step-growth polymerization of diols and telechelic polyethylenes with dicarboxylic acid end groups to synthesize PE-ester (Scheme 1B).[15,16] In step-growth polymerization, stoichiometric balance between alcohol and carboxylic acid groups is crucial for achieving high molar mass polymers. Even small deviations in the amounts of these functional groups can lead to the consumption of all limiting functional groups, resulting in a limited molar mass. This is

presumably why the ultimate strain for PE-esters was lower than that of HDPE, especially for the materials synthesized from low molar mass macromonomers, as reported by Arrington et al. Thus, it is important to develop a strategy to achieve perfect stoichiometry between two functional groups in step-growth polymerization to synthesize high molar mass PE-esters regardless of the molar mass of the initial macromonomers.

We have previously reported several examples of telechelic polyethylenes via ring-opening metathesis polymerization (ROMP) followed by hydrogenation in a tandem catalysis approach.[36–46] We demonstrated the efficient synthesis of dihydroxyl telechelic polyethylenes using a bioderived chain-transfer agent (CTA) with a long spacer between the hydroxy groups and the alkene. This approach eliminated the need for protection/deprotection in ROMP, resulting in improved atom economy.[36] Recently, Zhao et al. developed chemically recyclable polyethylenes synthesized through dehydrogenation of dihydroxyl telechelic polyethylenes catalyzed by ruthenium (Scheme 1C).[35] In this study, we synthesized telechelic polyethylenes with inherently stoichiometrically balanced ester and hydroxyl end groups. The equivalent number of ester and hydroxyl end groups are important to obtain a high degree of polymerization in subsequent step-growth polymerizations. The telechelic polyethylenes were generated using a new chain-transfer agent containing one ester and one hydroxyl group, with a long methylene spacer between the alkene group and the functional groups. Transesterification of these polyethylenes under neat conditions using a titanium catalyst resulted in colorless high molar mass PE-esters with a M_n of up to 111 kg/mol, which in turn exhibited competitive mechanical properties when compared to commercial polyethylenes (Scheme 1D). Changing the molar mass of oligomers between ester groups provided tunability of thermal and mechanical properties. These materials can be chemically recyclable through methanolysis of the PE-esters, followed by repolymerization.

We also envisioned that telechelic polyethylenes can be utilized to synthesize long chain branched PE-esters using a trifunctional compound to improve melt strength of linear PE-ester. Long chain branches denote branches exceeding the critical molar mass (M_c = 2~3*M_e, where M_e of PE = 1.2 kg/mol at 443 K), and thus able to form effective entanglements.[47] To the best of our knowledge, long chain branched HDPE using telechelic HDPE has been rarely reported. Recently, Arroyave *et al*. synthesized bifunctional and multifunctional telechelic HDPE from fragmenting post-consumer HDPE, and transesterification of these telechelic HDPE generated branched HDPE.[48] This pioneering work also demonstrated competitive tensile properties of the resulting polymers in comparison to HDPE. Here, we leveraged the inherent existence of two distinct end groups in the PE macromonomers to synthesize branched PE-esters using diethyl 5-(hydroxymethyl)isophthalate (DHIP) as a trifunctional compound (Scheme 1D). Transesterification of telechelic polyethylenes and DHIP successfully introduced long chain branching into PE-ester. The resulting branched polymer showed a similar elastic modulus but displayed higher melt strength during elongation compared to linear variants. This property is advantageous in various types of processing methods, including film-blowing and foaming.

Results and Discussion

Chain-Transfer Agent and Telechelic Polyethylene Macromonomers Syntheses

We prepared a chain-transfer agent (CTA) containing an alcohol and ester group at each end (Scheme 2). Ring-opening of oxacycloheptadec-10-en-2-one, known as ambrettolide under reflux conditions in methanol gave quantitative conversions (> 99%), determined by ^{1}H NMR spectroscopy, and high isolated yields (88%). The chemical structure of the CTA was analyzed by

^{1}H NMR spectroscopy, suggesting successful synthesis of the target molecule (Figure S16). This was further supported by mass spectrometry, which gave that $[M+Na]^+$ of 307.2301 g/mol, compared to the theoretical mass $[M+Na]^+_{theo}$ of 307.2249 g/mol.

The position of double bond was supported by mass spectrometry after cross metathesis with ethylene (i.e., ethenolysis). The cross metathesis reaction cleaved the internal double bond of the CTA to give two terminal olefins, resulting in $[M+NH_4]^+$ of 146.1537 and 202.1800, analyzed by gas chromatography-mass spectrometry (GC-MS) (Scheme S1 and Figure S1). These peaks are assigned to be M1 and M2, whose theoretical $[M+ NH_4]^+_{theo}$ values are 146.1545 and 202.1807, respectively. The chemical structure of the CTA was further supported by homonuclear correlation spectroscopy (COSY), and heteronuclear multiple bond correlation (HMBC) NMR spectroscopy (Figure S18 & S19).

Scheme 2. Synthesis of a Chain Transfer Agent, Linear and Branched PE-esters, and Chemical Recycling

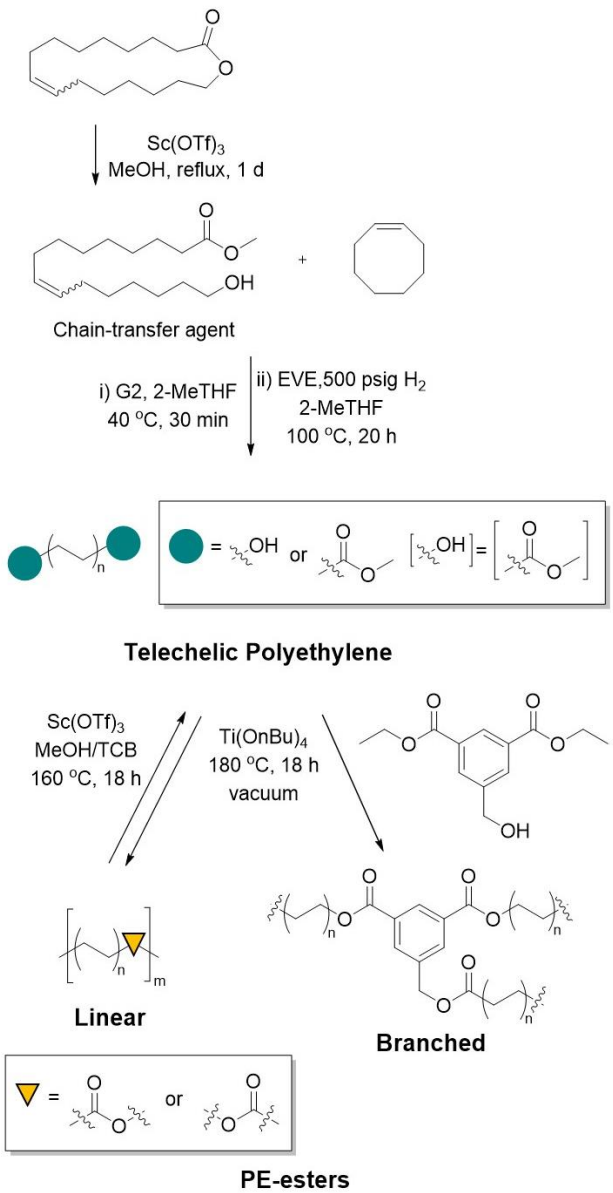

Extremely low Grubbs 2nd generation catalyst (G2) loading ($[G2]_0$:$[COE]_0$ = 1:20000, 0.005 mol%, 0.039 wt%, or 390 ppm relative to COE) was used to enable high end groups fidelity when $[COE]_0/[CTA]_0$ = 100. Even with the small amounts of G2 used, high conversion (>99%) of cyclooctene (COE) by ROMP in the presence of CTA was achieved in 30 min, determined by ^{1}H NMR spectroscopy. By changing $[COE]_0/[CTA]_0$ from 10 to 100, we were able to control M_n of the telechelic PCOEs from about 2 to 14 kg/mol (Table 1). The ester and hydroxyl groups were

incorporated in the same amounts, as supported by ^{1}H NMR spectroscopy after precipitation from methanol (Figure 1A). The end groups in the telechelic PCOEs were interrogated by matrix assisted laser desorption/ionization time-of-flight mass spectrometry (MALDI-TOF MS). The MALDI-TOF mass spectrum showed the PCOE peaks with hydroxyl-ester and ester-ester end groups (Figure S2). Hydroxyl-hydroxyl PCOE species were not observed in the MALDI analysis presumably due to ineffectual ionization processes, ion transmission, or ion detection.[49,50] Achieving exclusive heterotelechelic PCOEs requires regioselective reactions of the propagating species and the CTA in any intermolecular cross metathesis. Lack of regioselectivity in the chain transfer step is expected and the chain end groups are likely mixtures of ester–ester (1), hydroxyl–hydroxyl (1), and ester–hydroxyl (2).[51–53]

Table 1. Synthesis of Polyethylene Macromonomers and Linear PE-esters

ROMP and Hydrogenation										After transesterification			
Polymer	[COE] /[CTA]	PCOE		PE					Yield[d] (%)	Polymer	$M_{n,\,SEC}$[c] (kg/mol)	$M_{w,\,SEC}$[c] (kg/mol)	$Đ$[c]
		$Conv_{COE}$[a] (%)	$M_{n,\,NMR}$[a] (kg/mol)	Hydrogenation[b] (%)	$M_{n,\,NMR}$[b] (kg/mol)	$M_{n,\,SEC}$[c] (kg/mol)	$M_{w,\,SEC}$[c] (kg/mol)	$Đ$[c]					
PE-2k[e]	10	>99	1.8	97	1.8	1.6	2.2	1.4	75	PE_{2k}-93k	93	155	1.7
PE-9k[e]	50	99	6.0	99	4.8	8.9	11	1.2	87	PE_{9k}-101k	101	177	1.8
PE-16k	100	>99	14	97	12	16	22	1.3	92	PE_{16k}-111k	111	157	1.4

[a]Determined by ^{1}H NMR spectroscopy in $CDCl_3$. [b]Determined by ^{1}H NMR spectroscopy in toluene-d_8 at 100 °C. [c]Determined by 1,2,4-trichlorobenzene (TCB) SEC equipped with MALLS at 135 °C. [d]Obtained after filtration washed with DCM. [e]ROMP and hydrogenation were performed in toluene instead of 2-MeTHF.

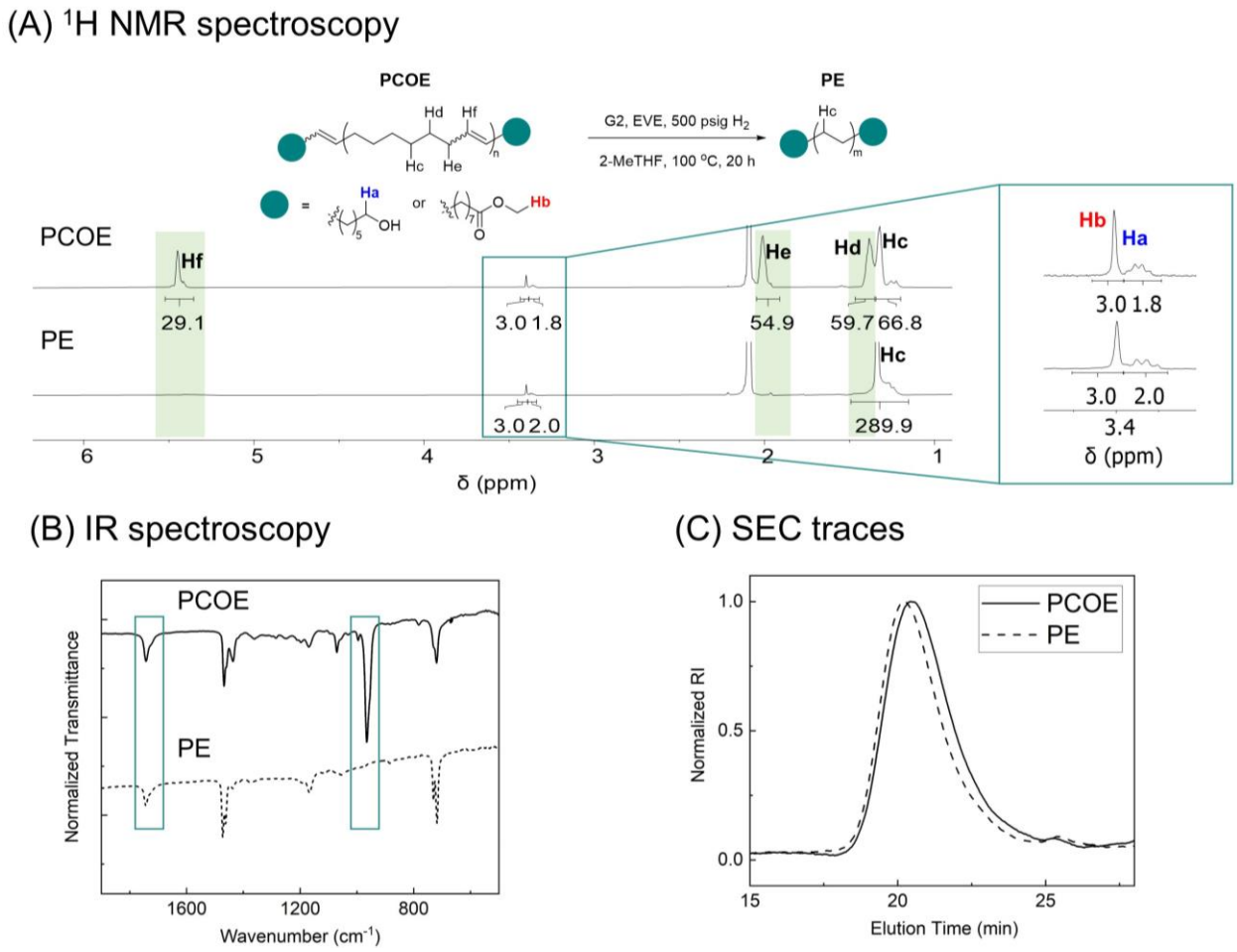

Figure 1. Characterizations of polycyclooctene (PCOE) and polyethylene (PE) macromonomers. (A) ^{1}H NMR spectra in toluene-d_8[a], (B) IR spectra[a], and (C) SEC traces in TCB at 135 °C[b]. [a]PCOE and PE macromonomer when [COE]/[CTA] = 10. [b]PCOE and PE macromonomer when $[COE]_0/[CTA]_0$ = 50.

Hydrogenation of polycyclooctene was performed in one-pot after adding ethyl vinyl ether and 2-MeTHF to the reaction mixtures after ROMP under 500 psig of H_2.[36,54–56] Based on ^{1}H NMR spectroscopy, 97–99% of alkenes were hydrogenated in all cases (Figure 1A and Table 1). Additionally, IR spectroscopy showed that C=C bending (964 cm^{-1}) was no longer evident, also indicating very high levels of hydrogenation (Figure 1B). Ester end groups remained in the polymer as determined by IR spectroscopy with a resonance at 1745 cm^{-1} and ^{1}H NMR

spectroscopy with a signal at 3.4 ppm, suggesting that ester groups were stable under these hydrogenation conditions (Figure 1A & B). Notably, ROMP and hydrogenation conditions maintained the equivalent amounts of ester and alcohol groups, supported by the integration ratios between Ha and Hb. This stoichiometric balance is important for the subsequent synthesis of high molar mass PE-esters. The SEC trace of telechelic PE remained relatively unchanged compared to PCOEs, suggesting that hydrogenation conditions did not significantly impact the molar mass (Figure 1C).

Synthesis of Linear and Branched PE-esters

Transesterification polymerizations were performed under vacuum at 180 °C to remove methanol and shift the equilibrium to the polymerized product. In the absence of the transesterification catalyst, molar mass only increased from 4.7 kg/mol to 6.5 kg/mol after transesterification (Table S1). Several catalysts, such as triazabicyclodecene (TBD), $Sn(Oct)_2$, $Ti(O^iPr)_4$, and $Ti(O^nBu)_4$, were investigated, with $Ti(O^nBu)_4$ giving the highest molar mass (M_n = 217 kg/mol) of PE-ester.[57] The SEC trace shifted to high molar mass, indicated by the shift towards earlier elution times with a small amount of remaining macromonomers and putative cyclic polymers (Figure 2). Moreover, a new signal appeared at 4.0 ppm in the ^{1}H NMR spectrum, assigned as methylene groups adjacent to the internal ester linkages (Figure S22 and S24). The two peaks from the end groups at 3.4 ppm were absent. These changes in ^{1}H NMR spectrum further supported the successful transesterification of telechelic polyethylene macromonomers.

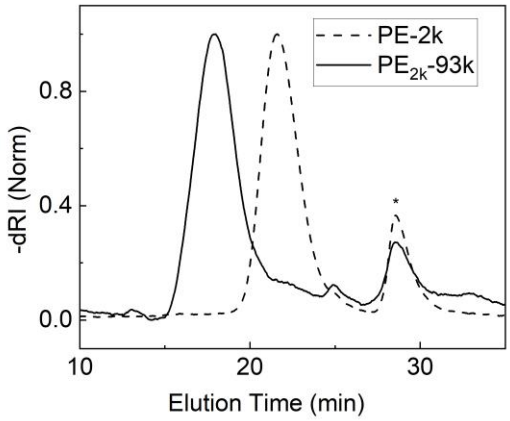

Figure 2. SEC traces in 1,2,4-trichlorobenzene at 135 °C of PE-2k and PE_{2k}-93k. Peak (*) observed at 29 minutes is an artifact associated with the SEC instrument.

The transesterification reaction was also performed on a 10 g scale, and polymerization of 16 kg/mol macromonomer resulted in high molar mass (M_n = 111 kg/mol, Table 1). Starting with lower molar mass macromonomers (2 and 9 kg/mol), polymerization provided 93 and 101 kg/mol of PE-ester, respectively. These findings suggested that the stoichiometrically self-balanced macromonomers generated high molar mass PE-esters, regardless of their initial molar mass. Additionally, lower molar mass macromonomers generated PE-esters with higher ester concentrations along the polymer backbone (higher [ester]/[1000 CH_2]).

We also synthesized branched PE-esters from transesterification polymerization of trifunctional DHIP and telechelic polyethylenes using $Ti(O^nBu)_4$ catalyst at 180 °C (Scheme 2 and Table 2). Under these reaction conditions, telechelic polyethylenes with a M_n of 12 kg/mol generated a branched polymer with a molar mass of 41 kg/mol of. Like linear PE-esters, the SEC trace of PE macromonomer was clearly shifted to a higher molar mass region (Figure S3). In ^1H NMR spectroscopy, new peaks appeared at 4.9 and 5.1 ppm, which are assigned to methylene protons next to phenyl ester groups and between phenyl and ester, respectively (Figure S26). These

peaks support the successful incorporation of DHIP to generate branched polymers. When 53 mol% of DHIP was added, the theoretical branching ratio, defined as the ratio of ester and hydroxyl groups from DHIP to all ester and hydroxyl groups, was 63%. The resulting polymers showed a branching ratio of 20%, defined as the ratio of ester groups from reacted DHIP to all reacted ester groups, as determined by ^{1}H NMR spectroscopy. We suspect this discrepancy stems from the low signal-to-noise in the ^{1}H NMR spectrum resulting from low contents of ester groups and low solubility of polymers. The gel fraction of the branched polymer, obtained through Soxhlet extraction in toluene for 2 days, was determined to be 2 wt%. Since the telechelic polyethylenes are mixtures of ester–ester, hydroxyl–hydroxyl, and ester–hydroxyl telechelic polyethylenes, it is likely that there are some loops and a small amount of cross-linked content.

Table 2. Synthesis of Branched PE-ester

Polymer	Telechelic PE			After transesterification			Branching Ratio[b] (%)	Gel fraction[c] (%)
	$M_{n,\,SEC}$[a] (kg/mol)	$M_{w,\,SEC}$[a] (kg/mol)	$Đ$[a]	$M_{n,\,SEC}$[a] (kg/mol)	$M_{w,\,SEC}$[a] (kg/mol)	$Đ$[a]		
B-PE$_{12k}$-41k	12	23	1.9	41	88	2.1	20	2

[a]Determined by TCB SEC equipped with MALLS at 135 °C. [b]Determined by ^{1}H NMR spectroscopy. [c]Obtained through Soxhlet extraction in toluene for 2 days, followed by overnight drying under vacuum.

Morphological and Thermal Characterization

We investigated crystalline structures of the telechelic polyethylene macromonomers and PE-esters using wide-angle x-ray scattering (WAXS). HDPE and poly(pentadecalactone) (PPDL) were also used as benchmarks for the low [ester]/[1000 CH_2] = 0 and high [ester]/[1000 CH_2] = 71 ratios, respectively (Figure 3).[58] Although WAXS patterns of PPDL was shifted compared to HDPE, those of telechelic polyethylenes, linear, and branched PE-esters are identical to that of HDPE. These results suggested that introduction of ester and hydroxyl groups into polyethylenes

at these small levels ([ester]/[1000 CH_2] < 8.4) still had the same crystalline packing, in good agreement with previous studies.[15,16,18,59–62]

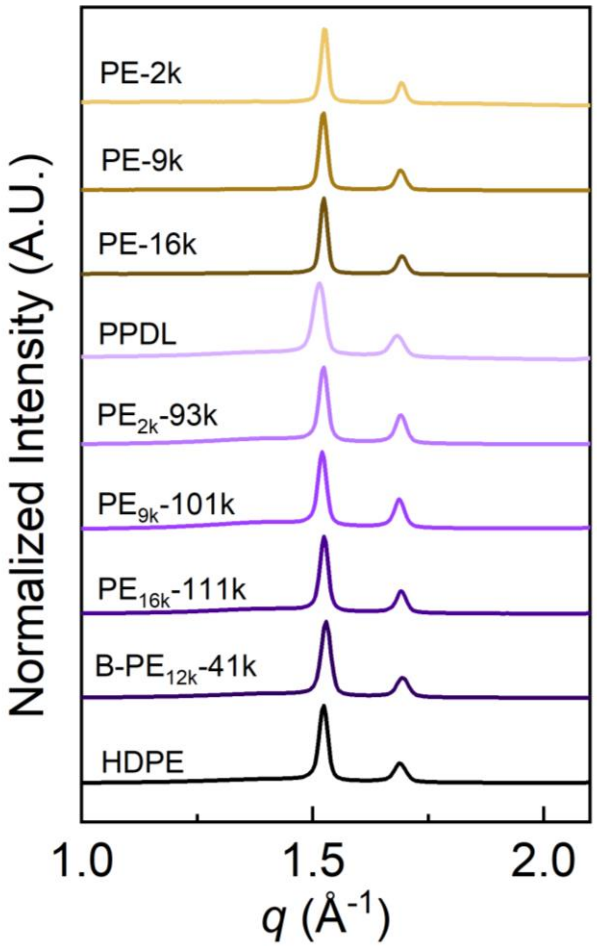

Figure 3. WAXS profiles of polyethylene macromonomers, PPDL, PE-esters, and HDPE.

We obtained the lamellar thickness from small-angle x-ray scattering (SAXS) for the samples by heating to 200 °C to erase thermal histories followed by cooling at 10 °C/min to –50 °C, 5 °C/min to –75 °C, and 2 °C/min to –90 °C. The lamellar thickness (L_m) was estimated from $L_m = X_c d^*$, where d^* is average distance between adjacent lamellae and X_c is degree of crystallinity obtained by differential scanning calorimetry (DSC).[63] For the macromonomers, higher molar mass samples had larger L_m values (Figure 4A, S4 and Table S3). PE-esters had even

larger L_m compared to the macromonomers, which was probably attributed to their higher molar mass. To determine whether ester groups were present in the crystalline domain or solely in the amorphous domain, we compared the L_m of the PE-esters with theoretical maximum length ($L_{PE,\ theo}$) between ester groups with fully extended with all *trans* conformation similar to that found in the PE crystal structure. For PE_{2k}-93k, L_m and $L_{PE,\ theo}$ were estimated to be 19 and 14 nm, respectively (Table S3). As the theoretical average length between ester groups was shorter than measured lamellar thickness, we conclude that at least some of the ester groups are likely embedded in the crystalline domains, and this finding agrees well with previous studies.[59,60]

To further support the incorporation of ester groups in the crystalline lamellae, we used IR spectroscopy. Certain infrared spectral regions can be distinguishable depending on whether functional groups are in the amorphous or crystalline phase due to different chain conformations.[64–66] To obtain samples with two different degrees of crystallinity in the same material, we utilized two different cooling rates after erasing thermal histories: one slowly cooled at 1 °C/min and the other rapidly cooled by quenching with liquid nitrogen. The slowly cooled sample exhibited a higher degree of crystallinity than the rapidly cooled one (Figure S5). In IR spectroscopy, the sample with higher crystallinity showed a more intense peak at 1725 cm^{-1} compared to the one with lower crystallinity (Figure S6). Therefore, it is likely that the peak at 1725 cm^{-1} is from ester groups in the crystalline domains. The peak was observed in both samples, suggesting that some ester groups were also included in the crystalline domain, even in the sample with lower crystallinity.

The decomposition temperature ($T_{d,\ 5\%}$), defined here as the temperature at which 5% mass loss of polymers occurs, was measured using thermogravimetric analysis (TGA) under an N_2 atmosphere to investigate the thermal stability of the polymers (Table 3). $T_{d,\ 5\%}$ of the polyethylene

macromonomers and the PE-esters were slightly lower than those of polyethylene, but their $T_{d,\,5\%}$ still remained high, ranging from 419 to 458 °C (Table 3). Thermal stability of PE_{2k}-93k under air was also tested. The sample was held at 200 °C for 10 and 60 minutes, respectively, after ramping up the temperature at a rate of 20 °C/min. Although TGA data showed less than 0.5% mass loss compared to initial mass (Figure S7), both samples changed color to a yellowish orange. Additionally, they became insoluble in 1,2,4-trichlorobenzene at 135 °C, suggesting cross-linking. This observation was also previously reported for HDPE when heating at 200 °C under air flow conditions.[67]

Table 3. Thermal Properties of Polyethylene Macromonomers, PPDL, Linear PE-esters, and HDPE

Polymer	[Ester]/[1000 CH_2]	$M_{n,\,SEC}$[a] (kg/mol)	$M_{w,\,SEC}$[a] (kg/mol)	$Đ$[a]	T_d[b] (°C)	T_m[c] (°C)	ΔH_m[c] (J/g)	T_c[d] (°C)	ΔH_c[d] (J/g)
PE-2k	7.2	1.6	2.2	1.4	421	126	284	113	292
PE-9k	2.9	8.9	11	1.2	422	132	264	118	273
PE-16k	1.5	16	22	1.3	447	134	253	119	239
PPDL	71.4	80	149	1.9	410	95	144	80	117
PE_{2k}-93k	8.4	93	155	1.7	458	131	156	106	165
PE_{9k}-101k	2.6	101	177	1.8	428	135	178	110	190
PE_{16k}-111k	0.9	111	157	1.4	419	135	176	112	185
B-PE_{12k}-41k	2.0	41	88	2.1	443	133	202	113	191
HDPE	0	46	89	1.9	485	132	191	115	189

[a]Determined by TCB SEC equipped with MALLS at 135 °C. [b]Temperature of 5% mass loss determined by TGA analysis at a heating rate of 10 °C/min under N_2 atmosphere. [c]Determined by DSC analysis under N_2 atmosphere at a heating rate of 10 °C/min based on the 2nd heating cycle. [d]Determined by DSC analysis under N_2 atmosphere at a cooling rate of 10 °C/min based on the 1st cooling cycle after deleting thermal history.

We also investigated the thermal properties using DSC. Interestingly, distinct trends were observed in the melting temperatures of the polyethylene macromonomers: higher molar mass polyethylene macromonomers melted at higher temperatures (Figure 4A and Table 3). The trend of T_m is correlated with that of L_m, suggesting that higher molar mass of macromonomers generated larger L_m, which in turn increased T_m.[68] Melting temperatures for linear PE-esters ranged from 131

to 135 °C (Figure 4B), and that of branched polymer was 133 °C, all similar to that of HDPE (132 °C, Table 3). In contrast, PPDL showed significantly lower T_m = 95 °C. These results indicated that [ester]/[1000 CH_2] = 8.4 in PE-ester was low enough to have a comparable T_m to HDPE while [ester]/[1000 CH_2] = 71.4 in PPDL was not.

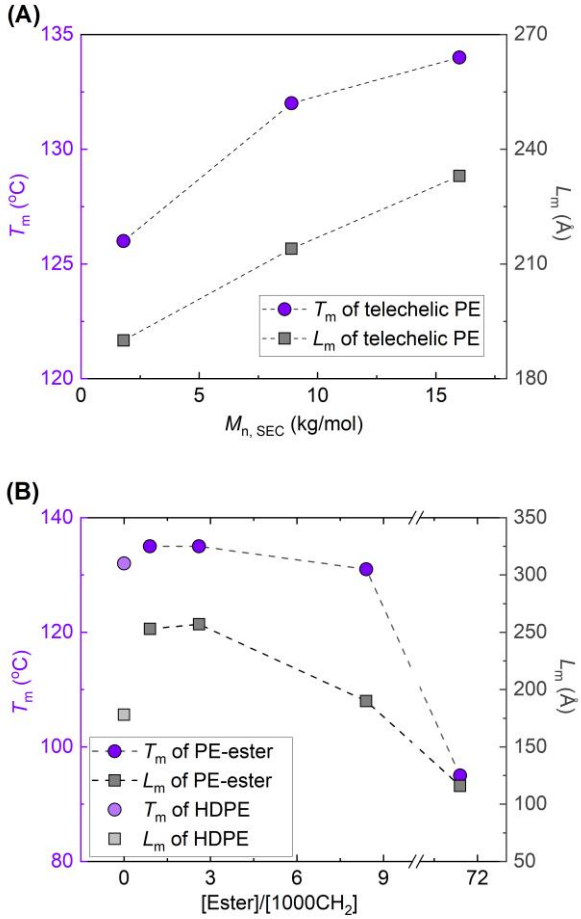

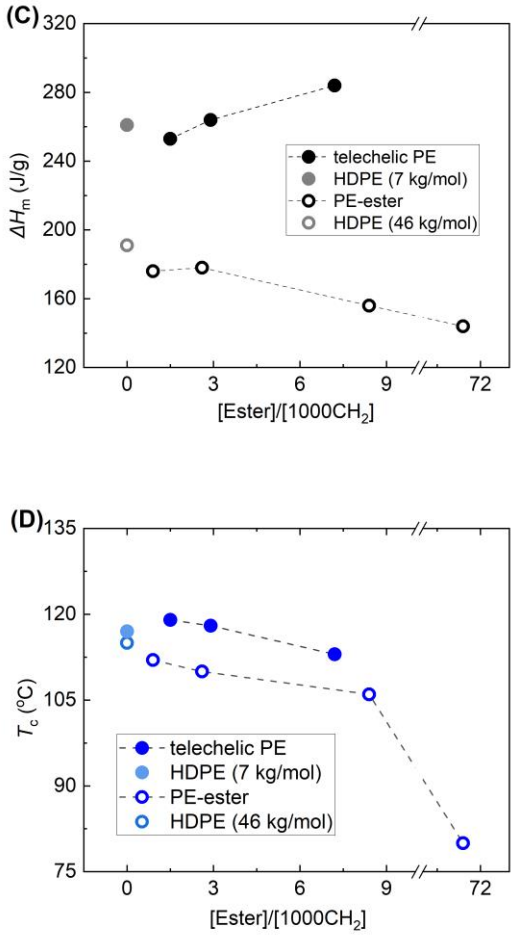

Figure 4. (A) T_m and L_m of telechelic macromonomers as a function of $M_{n,\,SEC}$ based on the 2nd heating cycle. **(B)** T_m and L_m of PPDL, PE-esters, and HDPE based on the 2nd heating cycle. **(C)** ΔH_m of PPDL, PE-esters, and HDPE based on the 2nd heating cycle. **(D)** T_c based on the 1st cooling cycle as a function of [ester]/[1000 CH_2] at a heating and a cooling rate of 10 °C/min after deleting thermal history.

The polyethylene macromonomers have higher enthalpies of melting compared to the PE-esters (Figure 4C and Table 3). To test if the larger ΔH_m is due to lower molar mass or to the presence of the macromonomers' functional groups, low molar mass HDPE (M_n = 7 kg/mol) was synthesized and its thermal properties were characterized. ΔH_m of low molar mass non-functional

HDPE was similar to that of macromonomers (Figure 4C). Furthermore, ΔH_m decreased as M_n increased in general (Figure S8). These results supported that the main factor for higher ΔH_m of macromonomers was their lower molar mass compared to the PE-esters. For PE-esters with [ester]/[1000 CH_2] ratios up to 2.6, their ΔH_m values were similar to HDPE with high molar mass. When [ester]/[1000 CH_2] was greater than 2.6, the ΔH_m values for the PE-esters began to decrease. Overall, considering T_m and ΔH_m started to decrease when [ester]/[1000 CH_2] was greater than 2.6, ester groups can be considered as defects in the crystal lattice of polyethylene.

Crystallization temperatures were also measured at a cooling rate of 10 °C/min after erasing thermal history. Polyethylene macromonomers crystallized at higher temperatures compared to PE-esters (Figure 4D and Table 3). Furthermore, low molar mass HDPE (M_n = 7 kg/mol) showed slightly higher T_c (117 °C) compared to high molar mass HDPE (115 °C, M_n = 46 kg/mol). Presumably, low molar mass macromonomers have more chain mobility at melt and thus begin nucleation at higher T_c than high molar mass PE-ester.[69,70] Generally, crystallization temperatures decreased as [ester]/[1000 CH_2] increased for each set of macromonomers and PE-esters. Branched PE-ester exhibited slightly higher crystallization temperature (113 °C) compared to their linear counterparts (106–112 °C). This behavior was also reported for long chain branched polypropylene, where the presence of branches could act as a heterogeneous nucleating agent, accelerating the polymer crystallization process.[71]

Mechanical Properties

Uniaxial tensile tests were performed to investigate mechanical properties of the synthesized polymers. Representative stress–strain curves of the PE-esters are shown in Figure 5

with HDPE and PPDL as benchmarks with zero ester and relatively high ester concentrations, respectively. The mechanical properties of PPDL and HDPE were well corroborated with previous reports.[12,15,16,18,72] All PE-esters showed competitive elongation at breaks ranging from 700 to 900% compared to HDPE (870%) (Figure 6A and Table S4).

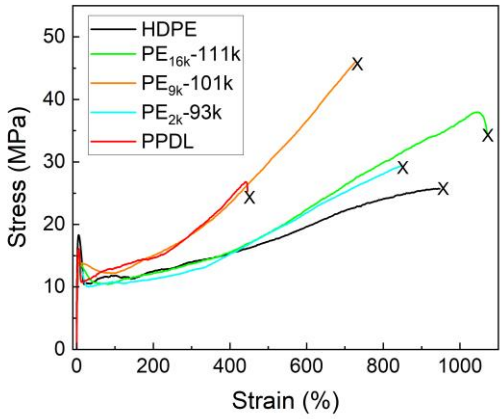

Figure 5. Representative stress–strain curves of PE-esters with commercial HDPE and PPDL as benchmarks, extended at 5 mm/min.

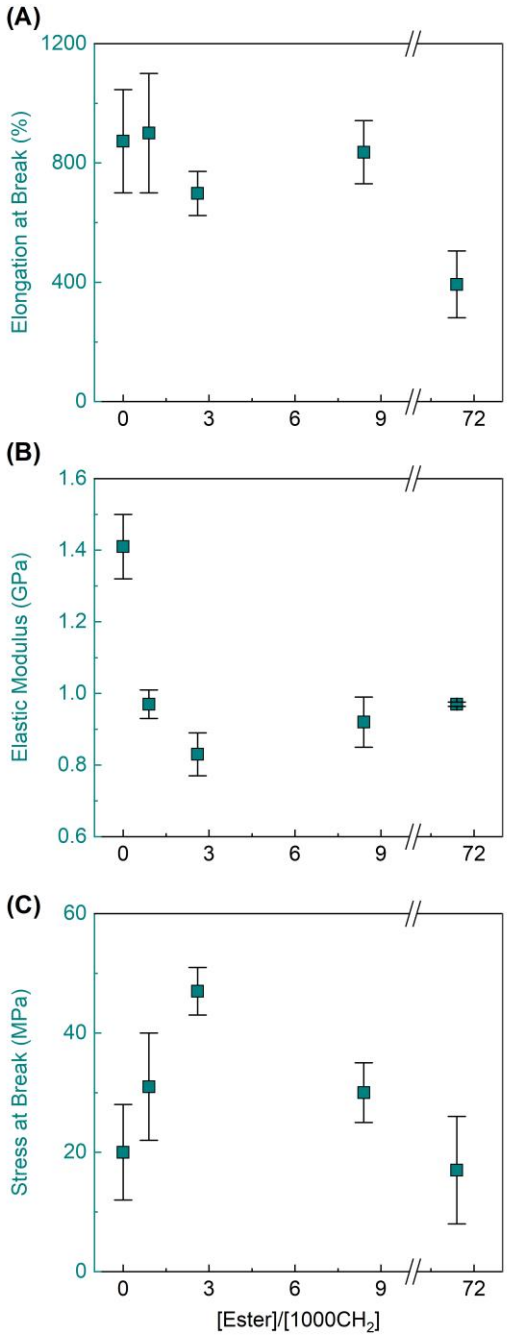

Figure 6. Mechanical properties of PE-esters with commercial HDPE and PPDL as benchmarks as a function of [Ester]/[1000 CH_2]: (A) elongation at break, (B) elastic modulus, and (C) stress at break. The squares and the error bars show average values and standard deviations, respectively, for at least 5 samples extended at 5 mm/min.

Elastic modulus was determined from the slope of the stress–strain curve in the linear viscoelastic regime. Shown in Figure 6B, elastic modulus decreased as the [ester]/[1000 CH_2] increased from 0 (HDPE) to 2.6 (PE_{9k}-101k). Then, the modulus slightly increased from PE_{9k}-101k to PPDL ([ester]/[1000 CH_2] = 2.6 to 71.4). The elastic modulus trend was well correlated with degree of crystallinity in the lower [ester]/[1000 CH_2] regime ranging from 0 to 8.4 (Figure S9). The elastic modulus of PPDL was maintained compared to other polymers, even though the degree of crystallinity decreased, presumably due to other factors, such as higher cohesive energy density resulting from the higher ester content.[73]

All linear polymer samples showed positive slopes after yielding, indicating strain induced hardening. This means that higher stress is required to further deform the plastics. To investigate the origin of the strain induced hardening, we measured the degree of crystallinity before and after elongation (Table S5). PE-esters and HDPE had higher degrees of crystallinity after elongation, suggesting strain-induced crystallization during elongation. Interestingly, stress at break increased until [ester]/[1000 CH_2] reached 2.6, and then decreased (Figure 6C). It has been reported that C-O bond is weaker than C-C bond, resulting in lower stress at break under deformation in PPDL.[72] The polar nature of the functional groups, molar mass, and degrees of crystallinity can also affect the materials' strength.[74–77] These multiple competing effects may have influenced the ultimate strength of the materials, and further investigations would be necessary to comprehensively understand this behavior.

The mechanical properties of branched PE-ester were also measured (Figure 7 and Table S7). To control the influence of molar mass on the mechanical properties, we synthesized M_n = 49 kg/mol of linear PE-esters (PE_{12k}-49k) and compared them with branched PE-esters (B-PE_{12k}-41k,

M_n = 41 kg/mol). Branched polymers exhibited ductility and elongation break at values ≈ 650%, which was comparable to that of HDPE. Moreover, compared to HDPE and linear PE-esters, the branched PE-ester displayed less strain-hardening, resulting in lower stress at break (Table S7). Interestingly, the degree of crystallinity of the branched PE-esters increased after elongation (Figure S11). Additionally, the elastic modulus of the material was 1.3 GPa, which is comparable to HDPE and higher than LDPE (Table S7). This can be attributed to the longer chain lengths between branching points in the branched PE-esters compared to LDPE.

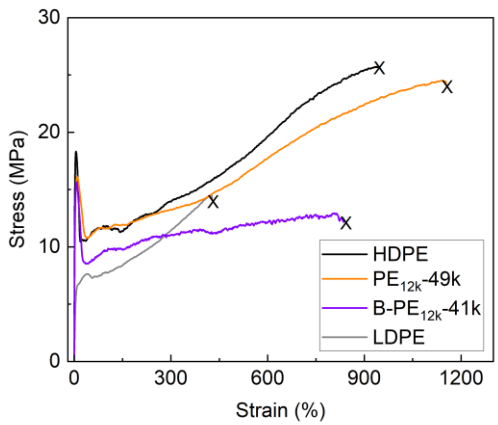

Figure 7. Representative stress–strain curves of linear and branched PE-esters with commercial HDPE and LDPE as benchmarks, extended at 5 mm/min.

After elongation, the testing regions of HDPE tensile bars were opaque and white while those of PPDL were still transparent (Figure S10). However, the whitening was observed only for the middle part of the PE-ester samples, not in the part near the grip. For the white parts, we observed more intense streaks along the equator in the 2D SAXS as compared to the transparent part which likely arose from long thin structures, such as fibrils formed during deformation.[78,79]

The formation of fibrils was further supported by scanning electron microscopy (SEM) (Figure S10). The white parts showed more apparent and densely packed fibrils than the transparent parts, which had much fewer fibrils.

Water vapor permeability

Water vapor permeability was measured for PE-esters as well as for reference materials such as HDPE and PPDL at relative humidities of 47–52% and a temperature of approximately 20 °C (Figure 8). Under these conditions, water vapor permeability of HDPE was 0.5 g mil/m^2 day kPa, and its reported value was 5.9 g mil/m^2 day kPa at relative humidity of 90% and a temperature of 40 °C.[80] This difference is likely due to variations in temperature and relative humidity conditions. PE-esters had slightly higher water vapor permeability (1.0–1.4 g mil/m^2 day kPa) than HDPE. PPDL had a water vapor permeability that was much higher (22 g mil/m^2 day kPa) compared to HDPE and PE-esters, presumably due to its lower degree of crystallinity and increased hydrophilicity compared to the other samples (Table S6). These results suggest that small amounts of ester groups ([Ester]/[1000 CH_2] < 10) are less likely to compromise the water vapor permeability of HDPE, while large amounts of ester groups ([Ester]/[1000 CH_2] = 71.4) lead to significant increases as observed in PPDL.

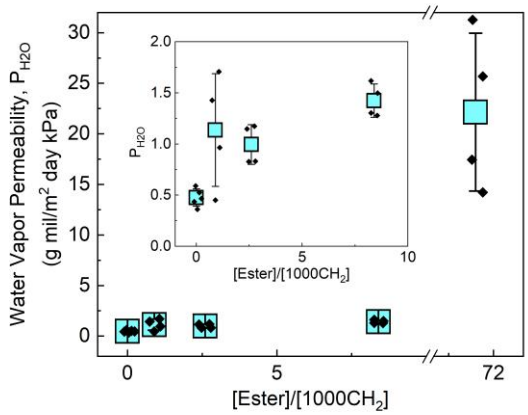

Figure 8. Water vapor permeability of HDPE, linear PE-esters, and PPDL.

Extensional Rheology

Melt-strain hardening is advantageous for melt processing methods, such as film blowing, foaming, and 3D printing, by limiting fracture behavior.[81,82] This phenomenon is known to be more prominent in branched melts. Extensional rheology of linear and branched samples was performed using an extensional viscosity fixture to investigate melt-strain hardening. The transient extensional viscosity was measured at 270 °C with various strain rates under nitrogen flow. Figure 9 shows the transient extensional viscosity (η_E^+) as a function of time (t). The extensional viscosity data collected at different strain rates all overlap well. This is expected behavior and supports the validity of the extensional measurements.

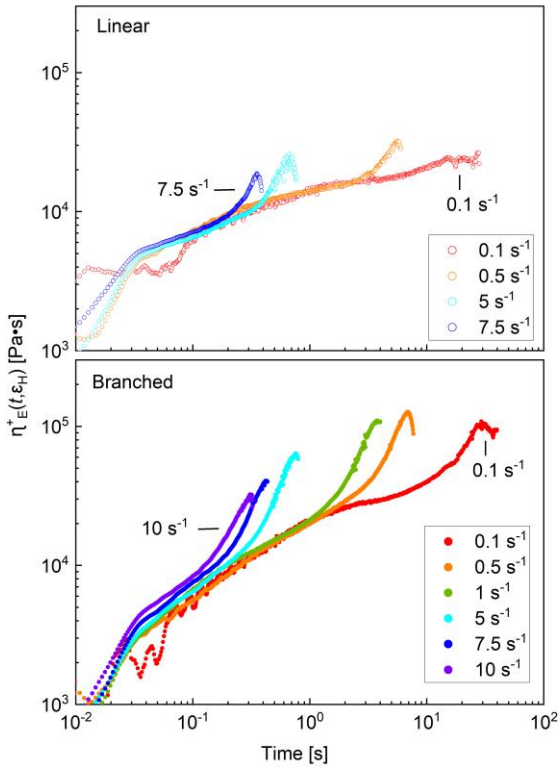

Figure 9. Transient extensional viscosity as a function of time for linear (PE_{12k}-49k) and branched (B-PE_{12k}-41k) polymers, taken at various strain rates. The graph was shown prior to the point where sudden decrease, which is the point where the samples failed.

Linear PE-esters showed slight melt-strain hardening that is likely associated with their high molar mass and entanglement density (Figure 9). Strain-hardening ratios (SHR) were calculated to quantify the extent of melt-strain hardening using the following equation, where $\eta_{E,LVE}^{+}(t)$ is defined as the transient extensional viscosity associated with the linear viscoelastic limit.

$$\text{SHR} = \eta_E^{+}(t, \dot{\varepsilon}_H) / \eta_{E,LVE}^{+}(t)$$

The data for $\eta_{E,LVE}^{+}(t)$ were taken as η_{E}^{+} at the lowest rate measured. In the case of the branched polymer, some non-linear viscoelastic flow is observed. However, this occurs at times longer than those associated with data taken at faster rates, so its approximation as $\eta_{E,LVE}^{+}(t)$ in the determination of the SHR is appropriate. When SHR is greater than 1, it indicates the presence of melt-strain hardening. Figure S13 plots the SHR as a function of time. The SHR of linear PE-esters were obtained up to 2.0. These values agree well with the reported SHR for commercial HDPE (SHR = 2 when strain rates were 0.1 and 1 s^{-1} at 160 °C).[83] That of branched PE-esters was observed up to SHR = 3.8 (Figure S13B). Based on the data, branching improves the melt-strain hardening behavior relative to the linear melt.[84] This finding is consistent with previous studies indicating that the introduction of long chain branching into polymers improves melt-strain hardening behavior.[85] This has been attributed to the pinned chain segments that exist between branching points. The branches effectively restrict the relaxation of these pinned segments, which greatly increases their relaxation time, resulting in melt strain hardening.

Chemical Recyclability of PE-esters

We investigated depolymerization of PE-esters into PE macromonomers by methanolysis catalyzed by $Sc(OTf)_3$. Depolymerization of PE-ester resulted in 9 kg/mol telechelic macromonomer and the SEC trace almost overlapped with the original PE (Figure 10 and Table S8). The slightly narrower dispersity compared to the original one is likely attributed to an artifact associated with polymer purification. In the ^{1}H NMR spectrum, the internal ester group peak at 4.0 ppm disappeared, and the methylene peak adjacent to terminal hydroxyl and the methyl ester peak at 3.4 ppm were regenerated. The equivalence between alcohol and ester end groups were maintained, supported by ^{1}H NMR spectroscopy (Figure S28). Then, we repolymerized the

recycled PE-9k under vacuum at 180 °C with $Ti(O^nBu)_4$ as catalyst, generating a colorless material with a M_n of 108 kg/mol of PE-esters.

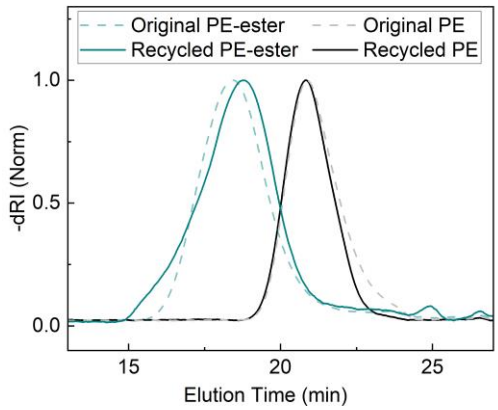

Figure 10. SEC traces of original and recycled PE and PE-ester.

Thermal and mechanical studies of recycled PE-ester were performed. T_m and T_c of recycled polymer were similar to that of original PE-esters (Table S9). The degree of crystallinity of recycled PE-ester was also comparable to the original one. The materials were still ductile and elongation at break was 260% although they failed earlier than the original PE-ester (Figure S14 and Table S4). The lower elongation at break compared to the virgin material is presumably due to fortuitous defects in the samples incorporated during reprocessing. Strain hardening was still observed, resulting in stress at break of 20 MPa. Elastic modulus and yield strength of recycled

polymers were like those of original polymers. These data demonstrate that PE-esters are chemically recyclable, and the recycled polymers still exhibit favorable properties.

Conclusions

We demonstrated a strategy to synthesize chemically recyclable high molar mass of linear and branched PE-esters from stoichiometrically self-balanced telechelic polyethylene macromonomers while maintaining the thermal and mechanical properties of HDPE. A chain-transfer agent with one ester and one hydroxyl group was developed to achieve stoichiometric balance between two functional groups. After ROMP and hydrogenation, this chain-transfer agent generated telechelic polyethylene macromonomers. Since the macromonomers had stoichiometrically balanced hydroxyl and ester end groups, step-growth polymerization of the macromonomers produced high molar mass of PE-ester up to $M_{n,SEC}$ = 111 kg/mol. By utilizing two distinct end groups in the macromonomers, we also synthesized long chain branched PE-ester using diethyl 5-(hydroxymethyl)isophthalate. Tuning [ester]/[1000 CH_2] ratio in the linear PE-esters, we systematically investigated the effects of introducing ester groups to HDPE on the resultant thermal and mechanical properties. Melting temperatures of these resulting polymers ranged from 131 to 135 °C which were comparable to commercial HDPE (T_m = 132 °C). Mechanical properties of the polymers were also competitive to HDPE. Branched PE-ester demonstrated a higher level of melt-strain hardening than the linear polymer, which is beneficial for melt processing methods, such as film blowing. The depolymerization of the PE-ester under methanolysis conditions regenerated telechelic polyethylene macromonomers. Repolymerization of these recycled polymers through transesterification produced high molar mass PE-ester (M_n = 108 kg/mol). These results provide a strategy to synthesize chemically recyclable alternatives to

HDPE, and a fundamental understanding of the ester group effects on the thermal, morphological, mechanical, and gas barrier properties of PE-esters.

Acknowledgement

We thank National Science Foundation Center for Sustainable Polymers at the University of Minnesota for financial support, which is a National Science foundation-supported Center for Chemical Innovation (CHE-1901635). We also thank Dr. Caitlin Sample, Dr. Aristotelis Zografos, and Daniel Krajovic for helpful discussion. We thank Dr. Adrian Amador, Dr. Hyung Kae Lee, and Dr. Sean Murray for providing PPDL, performing SEM, and GC-MS, respectively. WAXS and SAXS experiments were performed at the Sector 5 of the Advanced Photon Source at the DuPont-Northwestern-Dow Collaborative Access Team (DND-CAT) and Brookhaven National Laboratory. This was supported by E.I. DuPont de Nemours & Co., Northwestern University, and the U.S. DOE under contract no. DE-AC02-06CH11357 and CMS beamline of the National Synchrotron Light Source II, a U.S. Department of Energy (DOE) Office of Science User Facility operated for the DOE Office of Science by Brookhaven National Laboratory.

Supporting Information

Experimental and instrumental details, Optimization of polymerization data, ^{1}H and ^{13}C NMR spectroscopy, size exclusion chromatography data, thermal gravimetric analysis data, differential scanning calorimetry data, X-ray experiments data, mechanical properties data, water vapor permeability data, and extensional rheology data.

Data Access Statement

All primary data files are available free of charge in the Data Repository for the University of Minnesota (DRUM) at https://doi.org/10.13020/39me-vb21

Author Information

Corresponding Author

Marc A. Hillmyer - *Department of Chemistry, University of Minnesota, Minneapolis, MN 55455, USA*; *ORCID: 0000-0001-8255-3853* email: hillmyer@umn.edu

Authors

Yoon-Jung Jang - *Department of Chemistry, University of Minnesota, Minneapolis, MN 55455, USA. ORCID:* 0000-0002-2592-1733

Sam Nguyen - *Department of Chemistry, University of Minnesota, Minneapolis, MN 55455, USA.*

References

(1) Wang, Y.; Easteal, A. J.; Chen, X. D. Ethylene and Oxygen Permeability through Polyethylene Packaging Films. *Packag. Technol. Sci.* **1998**, *11* (4), 169–178. https://doi.org/10.1002/(SICI)1099-1522(199807/08)11:4<169::AID-PTS427>3.0.CO;2-Q.

(2) Gorrasi, G.; Maio, L. D.; Vittoria, V.; Acierno, D. Recycling Polyethylene from Automotive Fuel Tanks. *J. Appl. Polym. Sci.* **2002**, *86* (2), 347–351. https://doi.org/10.1002/app.10967.

(3) Paxton, N. C.; Allenby, M. C.; Lewis, P. M.; Woodruff, M. A. Biomedical Applications of Polyethylene. *Eur. Polym. J.* **2019**, *118*, 412–428. https://doi.org/10.1016/j.eurpolymj.2019.05.037.
(4) Westlie, A. H.; Chen, E. Y. -X.; Holland, C. M.; Stahl, S. S.; Doyle, M.; Trenor, S. R.; Knauer, K. M. Polyolefin Innovations toward Circularity and Sustainable Alternatives. *Macromol. Rapid Commun.* **2022**, 2200492. https://doi.org/10.1002/marc.202200492.
(5) Geyer, R.; Jambeck, J. R.; Law, K. L. Production, Use, and Fate of All Plastics Ever Made. *Sci. Adv.* **2017**, *3* (7), e1700782. https://doi.org/10.1126/sciadv.1700782.
(6) Borrelle, S. B.; Ringma, J.; Law, K. L.; Monnahan, C. C.; Lebreton, L.; McGivern, A.; Murphy, E.; Jambeck, J.; Leonard, G. H.; Hilleary, M. A.; Eriksen, M.; Possingham, H. P.; De Frond, H.; Gerber, L. R.; Polidoro, B.; Tahir, A.; Bernard, M.; Mallos, N.; Barnes, M.; Rochman, C. M. Predicted Growth in Plastic Waste Exceeds Efforts to Mitigate Plastic Pollution. *Science* **2020**, *369* (6510), 1515–1518. https://doi.org/10.1126/science.aba3656.
(7) Schyns, Z. O. G.; Shaver, M. P. Mechanical Recycling of Packaging Plastics: A Review. *Macromol. Rapid Commun.* **2021**, *42* (3), 2000415. https://doi.org/10.1002/marc.202000415.
(8) Ronca, S. Polyethylene. In *Brydson's Plastics Materials*; Elsevier, 2017; pp 247–278. https://doi.org/10.1016/B978-0-323-35824-8.00010-4.
(9) Odian, G. G. *Principles of Polymerization*, 4th ed.; Wiley-Interscience: Hoboken, N.J, 2004.
(10) Brahney, J.; Hallerud, M.; Heim, E.; Hahnenberger, M.; Sukumaran, S. Plastic Rain in Protected Areas of the United States. *Science* **2020**, *368* (6496), 1257–1260. https://doi.org/10.1126/science.aaz5819.
(11) Law, K. L.; Starr, N.; Siegler, T. R.; Jambeck, J. R.; Mallos, N. J.; Leonard, G. H. The United States' Contribution of Plastic Waste to Land and Ocean. *Sci. Adv.* **2020**, *6* (44), eabd0288. https://doi.org/10.1126/sciadv.abd0288.
(12) Arroyave, A.; Cui, S.; Lopez, J. C.; Kocen, A. L.; LaPointe, A. M.; Delferro, M.; Coates, G. W. Catalytic Chemical Recycling of Post-Consumer Polyethylene. *J. Am. Chem. Soc.* **2022**, jacs.2c11949. https://doi.org/10.1021/jacs.2c11949.
(13) Conk, R. J.; Hanna, S.; Shi, J. X.; Yang, J.; Ciccia, N. R.; Qi, L.; Bloomer, B. J.; Heuvel, S.; Wills, T.; Su, J.; Bell, A. T.; Hartwig, J. F. Catalytic Deconstruction of Waste Polyethylene with Ethylene to Form Propylene. *Science* **2022**, *377* (6614), 1561–1566. https://doi.org/10.1126/science.add1088.
(14) Kocen, A. L.; Cui, S.; Lin, T.-W.; LaPointe, A. M.; Coates, G. W. Chemically Recyclable Ester-Linked Polypropylene. *J. Am. Chem. Soc.* **2022**, *144* (28), 12613–12618. https://doi.org/10.1021/jacs.2c04499.
(15) Arrington, A. S.; Long, T. E. Influence of Carboxytelechelic Oligomer Molecular Weight on the Properties of Chain Extended Polyethylenes. *Polymer* **2022**, *259*, 125319. https://doi.org/10.1016/j.polymer.2022.125319.
(16) Arrington, A. S.; Brown, J. R.; Win, M. S.; Winey, K. I.; Long, T. E. Melt Polycondensation of Carboxytelechelic Polyethylene for the Design of Degradable Segmented Copolyester Polyolefins. *Polym. Chem.* **2022**, *13* (21), 3116–3125. https://doi.org/10.1039/D2PY00394E.
(17) Sullivan, K. P.; Werner, A. Z.; Ramirez, K. J.; Ellis, L. D.; Bussard, J. R.; Black, B. A.; Brandner, D. G.; Bratti, F.; Buss, B. L.; Dong, X.; Haugen, S. J.; Ingraham, M. A.; Konev, M. O.; Michener, W. E.; Miscall, J.; Pardo, I.; Woodworth, S. P.; Guss, A. M.; Román-Leshkov, Y.; Stahl, S. S.; Beckham, G. T. Mixed Plastics Waste Valorization through Tandem Chemical Oxidation and Biological Funneling. *Science* **2022**, *378* (6616), 207–211. https://doi.org/10.1126/science.abo4626.
(18) Häußler, M.; Eck, M.; Rothauer, D.; Mecking, S. Closed-Loop Recycling of Polyethylene-like Materials. *Nature* **2021**, *590* (7846), 423–427. https://doi.org/10.1038/s41586-020-03149-9.
(19) Coates, G. W.; Getzler, Y. D. Y. L. Chemical Recycling to Monomer for an Ideal, Circular Polymer Economy. *Nat. Rev. Mater.* **2020**, *5* (7), 501–516. https://doi.org/10.1038/s41578-020-0190-4.

(20) Boaen, N. K.; Hillmyer, M. A. Post-Polymerization Functionalization of Polyolefins. *Chem. Soc. Rev.* **2005**, *34* (3), 267. https://doi.org/10.1039/b311405h.
(21) Baur, M.; Lin, F.; Morgen, T. O.; Odenwald, L.; Mecking, S. Polyethylene Materials with In-Chain Ketones from Nonalternating Catalytic Copolymerization. *Science* **2021**, *374* (6567), 604–607. https://doi.org/10.1126/science.abi8183.
(22) Pepels, M. P. F.; Hansen, M. R.; Goossens, H.; Duchateau, R. From Polyethylene to Polyester: Influence of Ester Groups on the Physical Properties. *Macromolecules* **2013**, *46* (19), 7668–7677. https://doi.org/10.1021/ma401403x.
(23) Bouyahyi, M.; Pepels, M. P. F.; Heise, A.; Duchateau, R. ω-Pentandecalactone Polymerization and ω-Pentadecalactone/ε-Caprolactone Copolymerization Reactions Using Organic Catalysts. *Macromolecules* **2012**, *45* (8), 3356–3366. https://doi.org/10.1021/ma3001675.
(24) Zhao, R.; Zhang, Y.; Chung, J.; Shea, K. J. Convenient Controlled Aqueous C1 Synthesis of Long-Chain Aliphatic AB, AA, and BB Macromonomers for the Synthesis of Polyesters with Tunable Hydrocarbon Chain Segments. *ACS Macro Lett.* **2016**, *5* (7), 854–857. https://doi.org/10.1021/acsmacrolett.6b00427.
(25) Zhou, L.; Qin, P.; Wu, L.; Li, B.-G.; Dubois, P. Potentially Biodegradable "Short-Long" Type Diol-Diacid Polyesters with Superior Crystallizability, Tensile Modulus, and Water Vapor Barrier. *ACS Sustain. Chem. Eng.* **2021**, *9* (51), 17362–17370. https://doi.org/10.1021/acssuschemeng.1c06752.
(26) Marxsen, S. F.; Häußler, M.; Mecking, S.; Alamo, R. G. Unlayered–Layered Crystal Transition in Recyclable Long-Spaced Aliphatic Polyesters. *ACS Appl. Polym. Mater.* **2021**, *3* (10), 5243–5256. https://doi.org/10.1021/acsapm.1c01025.
(27) Nomura, K.; Binti Awang, N. W. Synthesis of Bio-Based Aliphatic Polyesters from Plant Oils by Efficient Molecular Catalysis: A Selected Survey from Recent Reports. *ACS Sustain. Chem. Eng.* **2021**, *9* (16), 5486–5505. https://doi.org/10.1021/acssuschemeng.1c00493.
(28) Roumanet, P.-J.; Jarroux, N.; Goujard, L.; Le Petit, J.; Raoul, Y.; Bennevault, V.; Guégan, P. Synthesis of Linear Polyesters from Monomers Based on 1,18-(*Z*)-Octadec-9-Enedioic Acid and Their Biodegradability. *ACS Sustain. Chem. Eng.* **2020**, *8* (45), 16853–16860. https://doi.org/10.1021/acssuschemeng.0c05671.
(29) Stempfle, F.; Ortmann, P.; Mecking, S. Long-Chain Aliphatic Polymers To Bridge the Gap between Semicrystalline Polyolefins and Traditional Polycondensates. *Chem. Rev.* **2016**, *116* (7), 4597–4641. https://doi.org/10.1021/acs.chemrev.5b00705.
(30) Naddeo, M.; D'Auria, I.; Viscusi, G.; Gorrasi, G.; Pellecchia, C.; Pappalardo, D. Tuning the Thermal Properties of Poly(Ethylene)-like Poly(Esters) by Copolymerization of E-caprolactone with Macrolactones, in the Presence of a Pyridylamidozinc(II) Complex. *J. Polym. Sci.* **2020**, *58* (4), 528–539. https://doi.org/10.1002/pol.20190085.
(31) Pepels, M. P. F.; Kleijnen, R. G.; Goossens, J. G. P.; Spoelstra, A. B.; Tandler, R.; Martens, H.; Soliman, M.; Duchateau, R. Compatibility and Epitaxial Crystallization between Poly(Ethylene) and Poly(Ethylene)-like Polyesters. *Polymer* **2016**, *88*, 63–70. https://doi.org/10.1016/j.polymer.2016.01.035.
(32) Maeda, T.; Kamimura, S.; Ohishi, T.; Takahara, A.; Otsuka, H. Synthesis of Polyethylene/Polyester Copolymers through Main Chain Exchange Reactions via Olefin Metathesis. *Polymer* **2014**, *55* (24), 6245–6251. https://doi.org/10.1016/j.polymer.2014.10.001.
(33) Roesle, P.; Stempfle, F.; Hess, S. K.; Zimmerer, J.; Río Bártulos, C.; Lepetit, B.; Eckert, A.; Kroth, P. G.; Mecking, S. Synthetic Polyester from Algae Oil. *Angew. Chem.* **2014**, *126* (26), 6918–6922. https://doi.org/10.1002/ange.201403991.
(34) Lebarbé, T.; Neqal, M.; Grau, E.; Alfos, C.; Cramail, H. Branched Polyethylene Mimicry by Metathesis Copolymerization of Fatty Acid-Based α,ω-Dienes. *Green Chem* **2014**, *16* (4), 1755–1758. https://doi.org/10.1039/C3GC42280A.

(35) Zhao, Y.; Rettner, E. M.; Harry, K. L.; Hu, Z.; Miscall, J.; Rorrer, N. A.; Miyake, G. M. Chemically Recyclable Polyolefin-like Multiblock Polymers. *Science* **2023**, *382* (6668), 310–314. https://doi.org/10.1126/science.adh3353.
(36) Sample, C. S.; Kellstedt, E. A.; Hillmyer, M. A. Tandem ROMP/Hydrogenation Approach to Hydroxy-Telechelic Linear Polyethylene. *ACS Macro Lett.* **2022**, *11* (5), 608–614. https://doi.org/10.1021/acsmacrolett.2c00144.
(37) Pitet, L. M.; Hillmyer, M. A. Carboxy-Telechelic Polyolefins by ROMP Using Maleic Acid as a Chain Transfer Agent. *Macromolecules* **2011**, *44* (7), 2378–2381. https://doi.org/10.1021/ma102975r.
(38) Todd, A. D.; McEneany, R. J.; Topolkaraev, V. A.; Macosko, C. W.; Hillmyer, M. A. Reactive Compatibilization of Poly(Ethylene Terephthalate) and High-Density Polyethylene Using Amino-Telechelic Polyethylene. *Macromolecules* **2016**, *49* (23), 8988–8994. https://doi.org/10.1021/acs.macromol.6b02080.
(39) Wang, H.; Onbulak, S.; Weigand, S.; Bates, F. S.; Hillmyer, M. A. Polyolefin Graft Copolymers through a Ring-Opening Metathesis Grafting through Approach. *Polym. Chem.* **2021**, *12* (14), 2075–2083. https://doi.org/10.1039/D0PY01728K.
(40) Martinez, H.; Zhang, J.; Kobayashi, S.; Xu, Y.; Pitet, L. M.; Matta, M. E.; Hillmyer, M. A. Functionalized Regio-Regular Linear Polyethylenes from the ROMP of 3-Substituted Cyclooctenes. *Appl. Petrochem. Res.* **2015**, *5* (1), 19–25. https://doi.org/10.1007/s13203-014-0048-z.
(41) Boaen, N. K.; Hillmyer, M. A. Selective and Mild Oxyfunctionalization of Model Polyolefins. *Macromolecules* **2003**, *36* (19), 7027–7034. https://doi.org/10.1021/ma0347621.
(42) Pitet, L. M.; Hillmyer, M. A. Combining Ring-Opening Metathesis Polymerization and Cyclic Ester Ring-Opening Polymerization To Form ABA Triblock Copolymers from 1,5-Cyclooctadiene and D,L-Lactide. *Macromolecules* **2009**, *42* (11), 3674–3680. https://doi.org/10.1021/ma900368a.
(43) Pitet, L. M.; Amendt, M. A.; Hillmyer, M. A. Nanoporous Linear Polyethylene from a Block Polymer Precursor. *J. Am. Chem. Soc.* **2010**, *132* (24), 8230–8231. https://doi.org/10.1021/ja100985d.
(44) Pitet, L. M.; Chamberlain, B. M.; Hauser, A. W.; Hillmyer, M. A. Synthesis of Linear, H-Shaped, and Arachnearm Block Copolymers By Tandem Ring-Opening Polymerizations. *Macromolecules* **2010**, *43* (19), 8018–8025. https://doi.org/10.1021/ma1014325.
(45) Kobayashi, S.; Kim, H.; Macosko, C. W.; Hillmyer, M. A. Functionalized Linear Low-Density Polyethylene by Ring-Opening Metathesis Polymerization. *Polym Chem* **2013**, *4* (4), 1193–1198. https://doi.org/10.1039/C2PY20883K.
(46) Kassekert, L. A.; Dingwell, C. E.; De Hoe, G. X.; Hillmyer, M. A. Processable Epoxy-Telechelic Polyalkenamers and Polyolefins for Photocurable Elastomers. *Polym. Chem.* **2020**, *11* (3), 712–720. https://doi.org/10.1039/C9PY01486A.
(47) Fetters, L. J.; Lohse, D. J.; Milner, S. T.; Graessley, W. W. Packing Length Influence in Linear Polymer Melts on the Entanglement, Critical, and Reptation Molecular Weights. *Macromolecules* **1999**, *32* (20), 6847–6851. https://doi.org/10.1021/ma990620o.
(48) Arroyave, A.; Cui, S.; Lopez, J. C.; Kocen, A. L.; LaPointe, A. M.; Delferro, M.; Coates, G. W. Catalytic Chemical Recycling of Post-Consumer Polyethylene. *J. Am. Chem. Soc.* **2022**, *144* (51), 23280–23285. https://doi.org/10.1021/jacs.2c11949.
(49) Altuntaş, E.; Weber, C.; Kempe, K.; Schubert, U. S. Comparison of ESI, APCI and MALDI for the (Tandem) Mass Analysis of Poly(2-Ethyl-2-Oxazoline)s with Various End-Groups. *Eur. Polym. J.* **2013**, *49* (8), 2172–2185. https://doi.org/10.1016/j.eurpolymj.2013.02.008.
(50) Nitsche, T.; Sheil, M. M.; Blinco, J. P.; Barner-Kowollik, C.; Blanksby, S. J. Electrospray Ionization-Mass Spectrometry of Synthetic Polymers Functionalized with Carboxylic Acid End-Groups. *J. Am. Soc. Mass Spectrom.* **2021**, *32* (8), 2123–2134. https://doi.org/10.1021/jasms.1c00085.

(51) Kobayashi, S.; Pitet, L. M.; Hillmyer, M. A. Regio- and Stereoselective Ring-Opening Metathesis Polymerization of 3-Substituted Cyclooctenes. *J. Am. Chem. Soc.* **2011**, *133* (15), 5794–5797. https://doi.org/10.1021/ja201644v.
(52) Martinez, H.; Ren, N.; Matta, M. E.; Hillmyer, M. A. Ring-Opening Metathesis Polymerization of 8-Membered Cyclic Olefins. *Polym. Chem.* **2014**, *5* (11), 3507. https://doi.org/10.1039/c3py01787g.
(53) Radlauer, M. R.; Matta, M. E.; Hillmyer, M. A. Regioselective Cross Metathesis for Block and Heterotelechelic Polymer Synthesis. *Polym. Chem.* **2016**, *7* (40), 6269–6278. https://doi.org/10.1039/C6PY01231K.
(54) Drouin, S. D.; Zamanian, F.; Fogg, D. E. Multiple Tandem Catalysis: Facile Cycling between Hydrogenation and Metathesis Chemistry. *Organometallics* **2001**, *20* (26), 5495–5497. https://doi.org/10.1021/om010747d.
(55) Yoon, K.-H.; Kim, K. O.; Wang, C.; Park, I.; Yoon, D. Y. Synthesis and Structure-Property Comparisons of Hydrogenated Poly(Oxanorbornene-Imide)s and Poly(Norbornene-Imide)s Prepared by Ring-Opening Metathesis Polymerization. *J. Polym. Sci. Part Polym. Chem.* **2012**, *50* (18), 3914–3921. https://doi.org/10.1002/pola.26171.
(56) Camm, K. D.; Martinez Castro, N.; Liu, Y.; Czechura, P.; Snelgrove, J. L.; Fogg, D. E. Tandem ROMP−Hydrogenation with a Third-Generation Grubbs Catalyst. *J. Am. Chem. Soc.* **2007**, *129* (14), 4168–4169. https://doi.org/10.1021/ja071047o.
(57) DeRosa, C. A.; Kua, X. Q.; Bates, F. S.; Hillmyer, M. A. Step-Growth Polyesters with Biobased (*R*)-1,3-Butanediol. *Ind. Eng. Chem. Res.* **2020**, *59* (35), 15598–15613. https://doi.org/10.1021/acs.iecr.0c03009.
(58) Amador, A. G.; Watts, A.; Neitzel, A. E.; Hillmyer, M. A. Entropically Driven Macrolide Polymerizations for the Synthesis of Aliphatic Polyester Copolymers Using Titanium Isopropoxide. *Macromolecules* **2019**, *52* (6), 2371–2383. https://doi.org/10.1021/acs.macromol.9b00065.
(59) Ortmann, P.; Mecking, S. Long-Spaced Aliphatic Polyesters. *Macromolecules* **2013**, *46* (18), 7213–7218. https://doi.org/10.1021/ma401305u.
(60) Menges, M. G.; Penelle, J.; Le Fevere de Ten Hove, C.; Jonas, A. M.; Schmidt-Rohr, K. Characterization of Long-Chain Aliphatic Polyesters: Crystalline and Supramolecular Structure of PE22,4 Elucidated by X-Ray Scattering and Nuclear Magnetic Resonance. *Macromolecules* **2007**, *40* (24), 8714–8725. https://doi.org/10.1021/ma071590p.
(61) Inci, B.; Lieberwirth, I.; Steffen, W.; Mezger, M.; Graf, R.; Landfester, K.; Wagener, K. B. Decreasing the Alkyl Branch Frequency in Precision Polyethylene: Effect of Alkyl Branch Size on Nanoscale Morphology. *Macromolecules* **2012**, *45* (8), 3367–3376. https://doi.org/10.1021/ma3002577.
(62) Few, C. S.; Wagener, K. B.; Thompson, D. L. Systematic Studies of Morphological Changes of Precision Polyethylene. *Macromol. Rapid Commun.* **2014**, *35* (2), 123–132. https://doi.org/10.1002/marc.201300672.
(63) Pérez-Camargo, R. A.; d'Arcy, R.; Iturrospe, A.; Arbe, A.; Tirelli, N.; Müller, A. J. Influence of Chain Primary Structure and Topology (Branching) on Crystallization and Thermal Properties: The Case of Polysulfides. *Macromolecules* **2019**, *52* (5), 2093–2104. https://doi.org/10.1021/acs.macromol.8b02659.
(64) Praveena, N. M.; Shaiju, P.; Raj, R. B. A.; Gowd, E. B. Infrared Bands to Distinguish Amorphous, Meso and Crystalline Phases of Poly(Lactide)s: Crystallization and Phase Transition Pathways of Amorphous, Meso and Co-Crystal Phases of Poly(L-Lactide) in the Heating Process. *Polymer* **2022**, *240*, 124495. https://doi.org/10.1016/j.polymer.2021.124495.
(65) Huy, T. A.; Adhikari, R.; Lüpke, T.; Henning, S.; Michler, G. H. Molecular Deformation Mechanisms of Isotactic Polypropylene in α- and β-Crystal Forms by FTIR Spectroscopy: Molecular Deformation of α-/β-Crystal iPP. *J. Polym. Sci. Part B Polym. Phys.* **2004**, *42* (24), 4478–4488. https://doi.org/10.1002/polb.20117.

(66) Qian, C.; Zhao, Y.; Wang, Z.; Liu, L.; Wang, D. Probing the Difference of Crystalline Modifications and Structural Disorder of Isotactic Polypropylene via High-Resolution FTIR Spectroscopy. *Polymer* **2021**, *224*, 123722. https://doi.org/10.1016/j.polymer.2021.123722.
(67) Cuadri, A. A.; Martín-Alfonso, J. E. The Effect of Thermal and Thermo-Oxidative Degradation Conditions on Rheological, Chemical and Thermal Properties of HDPE. *Polym. Degrad. Stab.* **2017**, *141*, 11–18. https://doi.org/10.1016/j.polymdegradstab.2017.05.005.
(68) Hiemenz, P. C.; Lodge, T. *Polymer Chemistry*, 2nd ed.; CRC Press: Boca Raton, 2007.
(69) Androsch, R.; Di Lorenzo, M. L.; Schick, C. Effect of Molar Mass on Enthalpy Relaxation and Crystal Nucleation of Poly (l-Lactic Acid). *Eur. Polym. J.* **2017**, *96*, 361–369. https://doi.org/10.1016/j.eurpolymj.2017.08.058.
(70) Ergoz, E.; Fatou, J. G.; Mandelkern, L. Molecular Weight Dependence of the Crystallization Kinetics of Linear Polyethylene. I. Experimental Results. *Macromolecules* **1972**, *5* (2), 147–157. https://doi.org/10.1021/ma60026a011.
(71) Tian, J.; Yu, W.; Zhou, C. Crystallization Behaviors of Linear and Long Chain Branched Polypropylene. *J. Appl. Polym. Sci.* **2007**, *104* (6), 3592–3600. https://doi.org/10.1002/app.26024.
(72) Cai, J.; Liu, C.; Cai, M.; Zhu, J.; Zuo, F.; Hsiao, B. S.; Gross, R. A. Effects of Molecular Weight on Poly(ω-Pentadecalactone) Mechanical and Thermal Properties. *Polymer* **2010**, *51* (5), 1088–1099. https://doi.org/10.1016/j.polymer.2010.01.007.
(73) Lee, C. J. Correlations of Elastic Modulus, Cohesive Energy Density and Heat Capacity Jump of Glassy Polymers. *Polym. Eng. Sci.* **1987**, *27* (13), 1015–1017. https://doi.org/10.1002/pen.760271314.
(74) Haward, R. N. Strain Hardening of Thermoplastics. *Macromolecules* **1993**, *26* (22), 5860–5869. https://doi.org/10.1021/ma00074a006.
(75) Thuy, M.; Pedragosa-Rincón, M.; Niebergall, U.; Oehler, H.; Alig, I.; Böhning, M. Environmental Stress Cracking of High-Density Polyethylene Applying Linear Elastic Fracture Mechanics. *Polymers* **2022**, *14* (12), 2415. https://doi.org/10.3390/polym14122415.
(76) Physical, Thermal, and Mechanical Properties of Polymers. In *Biosurfaces*; John Wiley & Sons, Inc: Hoboken, NJ, USA, 2015; pp 329–344. https://doi.org/10.1002/9781118950623.app1.
(77) Walkowiak, K.; Irska, I.; Zubkiewicz, A.; Rozwadowski, Z.; Paszkiewicz, S. Influence of Rigid Segment Type on Copoly(Ether-Ester) Properties. *Materials* **2021**, *14* (16), 4614. https://doi.org/10.3390/ma14164614.
(78) Afeworki, M.; Brant, P.; Lustiger, A.; Norman, A. Solid-State 13C NMR and Synchrotron SAXS/WAXS Studies of Uniaxially-Oriented Polyethylene. *Solid State Nucl. Magn. Reson.* **2015**, *72*, 27–40. https://doi.org/10.1016/j.ssnmr.2015.10.003.
(79) Cai, J.; Hsiao, B. S.; Gross, R. A. Real-Time Structure Changes during Uniaxial Stretching of Poly(ω-Pentadecalactone) by *in Situ* Synchrotron WAXD/SAXS Techniques. *Macromolecules* **2011**, *44* (10), 3874–3883. https://doi.org/10.1021/ma102949h.
(80) Wu, F.; Misra, M.; Mohanty, A. K. Challenges and New Opportunities on Barrier Performance of Biodegradable Polymers for Sustainable Packaging. *Prog. Polym. Sci.* **2021**, *117*, 101395. https://doi.org/10.1016/j.progpolymsci.2021.101395.
(81) Weingart, N.; Raps, D.; Lu, M.; Endner, L.; Altstädt, V. Comparison of the Foamability of Linear and Long-Chain Branched Polypropylene—The Legend of Strain-Hardening as a Requirement for Good Foamability. *Polymers* **2020**, *12* (3), 725. https://doi.org/10.3390/polym12030725.
(82) Münstedt, H.; Steffl, T.; Malmberg, A. Correlation between Rheological Behaviour in Uniaxial Elongation and Film Blowing Properties of Various Polyethylenes. *Rheol. Acta* **2005**, *45* (1), 14–22. https://doi.org/10.1007/s00397-005-0435-6.
(83) Morelly, S. L.; Alvarez, N. J. Characterizing Long-Chain Branching in Commercial HDPE Samples via Linear Viscoelasticity and Extensional Rheology. *Rheol. Acta* **2020**, *59* (11), 797–807. https://doi.org/10.1007/s00397-020-01233-5.

(84) Zografos, A.; All, H. A.; Chang, A. B.; Hillmyer, M. A.; Bates, F. S. Star-to-Bottlebrush Transition in Extensional and Shear Deformation of Unentangled Polymer Melts. *Macromolecules* **2023**, *56* (6), 2406–2417. https://doi.org/10.1021/acs.macromol.3c00015.
(85) McLeish, T. C. B.; Larson, R. G. Molecular Constitutive Equations for a Class of Branched Polymers: The Pom-Pom Polymer. *J. Rheol.* **1998**, *42* (1), 81–110. https://doi.org/10.1122/1.550933.

TOC graphic

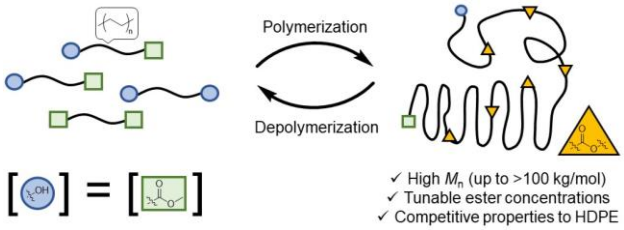
Polymerization
Depolymerization
✓ High M_n (up to >100 kg/mol)
✓ Tunable ester concentrations
✓ Competitive properties to HDPE